Structural Eng. / Earthquake Eng. Vol. 3. No. 1, 167 s-174 s, April 1986
Japan Society of Civil Engineers (Proc. of JSCE No. 368/ I -5)

THE ROLE OF END PLATES IN TWO DIMENSIONAL WIND TUNNEL TESTS

By Yoshinobu KUBO and Kusuo KATO***

End plates have been used for two-dimensional aerostatic and aerodynamic wind tunnel tests. Although it is often discussed that there exists the optimum size of end plates to create a two-dimensional air flow on testing body in wind tunnel tests, the mechanism of end plate effects is not yet made clear in detail. This paper discusses the mechanism of end plate effects from various view points by measuring drag forces, base pressure distributions, wind velocity distributions around the testing body and flow visualization by hydrogen bubble techniques for the flat plate normal to flow. It is concluded that the diameter required for the circular end plates has the relation with the wake vortex formation region and it is larger than 8 times of the testing body depth normal to flow.

1. INTRODUCTION

End plates have been used for two-dimensional wind tunnel tests in investigation of aerodynamic and aerostatic characteristics of bridges and buildings. The accurate estimation of air forces for structures is very important for the design of long span bridges and high rise buildings. If the design load is underestimated, the bridges and buildings are put in over-loaded conditions and it brings about breakdowns of these structures. The choice of the optimum size of end plates offers one of the keys for accurate estimation of the air forces applied to structures in case of air forces are estimated by using two dimensional wind tunnel tests. But the role of end plates had not been investigated in detail. Nakaguchi[1] pointed out from his research about the aerostatic drag forces of square and circular cylinders that the magnitude of aerostatic drag forces depends on the diameter of circular end plates. But he did not detail the mechanism of end plate effects. Takada[2] progressed his research by concentrating his attention on the two dimensional characteristics of base pressure distribution of normal flat plates (means flat plate normal to flow) with end plates of various diameters. But he did not detail the occurrence process of this phenomenon, either.

The present paper discusses the fundamental mechanism of the dependency of drag forces on the end plate diameter from the view point of air flow condition around testing body. As a normal flat plate has been often used[3)~8)] for a basic research about wake vortex condition, blockage effect and end plates effects and so on, this body is very convenient from the view point of that the accuracy of experimented data in the present study can be compared easily with that of another studies. In order to investigate the mechanism of end plates effects, the normal flat plate is chosen as the testing body and the base pressure distributions

* Member of JSCE, Dr. Eng., Assoc. Prof. of Civil Eng., Kyushu Institute of Technology (Tobata, Kitakyushu)
** Member of JSCE, Assistant of Civil Eng., Kyushu Institute of Technology (Tobata, Kitakyushu)

and the wind velocity distributions in the wake are measured and the flow patterns are visualized by using hydrogen bubble visualization techniques.

2. EXPERIMENTAL METHODS

The experiments were done by using the open circuit type wind tunnel with the square test section of 107 ×107(cm), which belongs to Dept. of Civil Engineering of Kyushu Institute of Technology.

The testing body was supported by the sensing element plates with gauges for measurement of drag forces. The end plates of testing body were separated from the testing body and was supported on the wind tunnel walls by the covers for sensing element plates not to measure the drag forces of the end plates and the sensing element plates (refer to Fig. 1). The circular and the airfoil shapes were chosen as those of covers for the sensing element plates. The testing body is aluminium plate with length of 79 cm, depth of 4 cm, thickness of 2 mm. The end plates are circular disks and the diameters are 4, 5, 6, 7, 8, 9, 10, 11, 12, 13, 14, 15, 16 times of depth of the testing body. They had thickness of 10 mm, edges of 45 deg. and cocentric circle holes of 60 mm diameter.

Fig. 2 shows the definition of coordinates in the present measuring system. X-axis is flow direction, Y-axis is model axis and Z-axis is vertical direction. The origin is center of model.

The traverse equipment controlled by the micro computer was used to enable to move X-type hot wire probes to the setting position within the expected accuracy. This equipment has the moving accuracy of 0.25 mm for horizontal, 0.0125 mm for vertical and 0.125 deg. for rotation.

3. INFLUENCE OF FLOW CONDITION OUT OF END PLATES

The covers for sensing element plates were used to get rid of sensing the air forces applied to the sensing element plates which were set between testing body and wind tunnel walls. Fig. 3 shows the shapes of the circular type cover with diameter of 65 mm and of the airfoil type cover of NACA 0020 with 65 mm at the thick of it. Fig. 4 shows the results of the measured drag forces of the normal flat plate with two different shape covers in the case of $D/d=4$. The measured drag force coefficients of the normal flat plate with the circular type cover get relatively large values and fluctuate to the various wind velocities, but those with the airfoil type cover do not fluctuate and get constant values to various wind velocities. The fluctuation of the measured drag forces in the case of the circular type cover is supposed to be caused by the wake vortexes of the circular type cover which influences the wake formation of the normal flat plates. Although it is considered that the characteristics of Fig. 4 depend on the sizes of the covers and the end plates, the airfoil type cover was used for the present experiments based on these results.

4. DRAG FORCES AND DIAMETER OF END PLATES

Fig. 5 shows the relation between the measured drag force coefficients (C_d) and the ratio (D/d) of the end plate diameter (D) to the testing body depth (d). C_d gets the value of 1.91 at $D/d=4$, but gets about

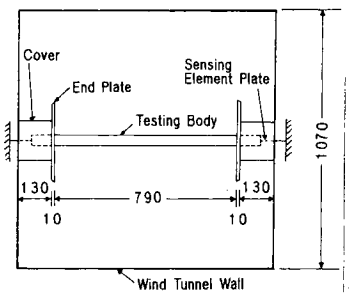

Fig. 1 Testing body mounting system.

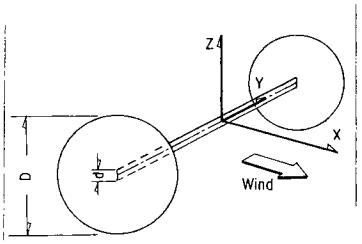

Fig. 2 Coordinates of testing system.

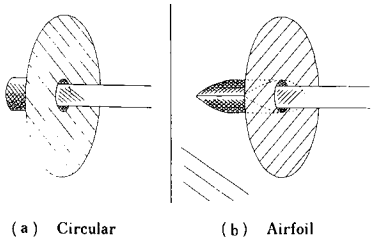

Fig. 3 Shapes of supporting cover.

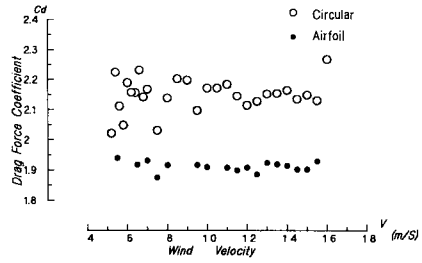

Fig. 4 Drag force coefficients of normal flat plate due to shapes of supporting cover.

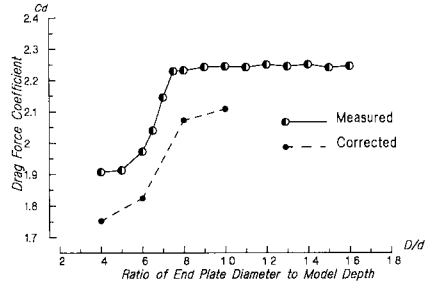

Fig. 5 Drag force coefficients of normal flat plate with various diameters of end plates.

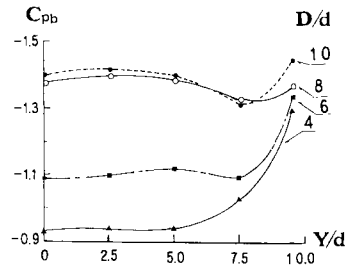

Fig. 6 Base pressure distributions of normal flat plate with various diameters of end plates.

2.25 at $D/d>8$. There exists the drastic change of the drag forces between $D/d=4$ and $D/d=8$. It is assumed that the air flow around the testing body has the drastic change between two end plate ratios. The main purpose of this paper is to make clear the cause of this drastic change of the drag forces. The size of usual end plates is around 5 or 6 times of the representative model length. This causes about 20 % error in the measured value to the true value. Adding to this, the blockage effects should be investigated on checking the accuracy of the measured drag forces. The broken line in Fig. 5 shows the corrected values which are calculated based on Maskel's equations for the blockage effect by using the base pressure.

Maskel[4] reported the drag force coefficient of the normal flat plate as $C_d=1.86$ which is corrected by the equations for correction of blockage effect from Fage & Johansen's experimental results[3] of $C_d=2.13$ in the blockage ratio of 7.15 %. According to Fig. 5, this correction value corresponds to the value for $D/d=6.5$. It is supposed that Fage & Johansen used the end plates of about $D/d=6.5$. The true value is estimated as $C_d=2.108$ by averaging the corrected values by applying the correction equations for the blockage effects to the present study results which are experimented in the condition of the end plate diameter $D>8\,d$ and the blockage ratio of 3.74 %. Comparing with the corrected value of Fage & Johansen's results, the author's corrected value is more reasonable as the value of drag force coefficient of the normal flat plate in two dimensional wind tunnel tests.

5. BASE PRESSURE DISTRIBUTION

The base pressure distributions were measured in the cases of the end plates of $D/d=4$, 6, 8 and 10 as shown in Fig. 6. This shows that the base pressure values at center ($Y/d=0$) of the testing body corresponds well to the drag force to each end plate diameter. Takada pointed out that the loss of two dimensionality of the base pressure distribution in spanwise direction is main cause for the decrement of absolute value of the base pressure with decrement of diameters of the end plates. The important point in this data is the difference of the base pressure magnitude at center part of the testing body. As it is considered that the difference of the pressure values at $Y/d=0$ remarkably relates with the end plate diameters. The things investigated are to make clear the reason why the absolute magnitudes of the base pressure at center part decrease with decrement of the end plate diameter and get almost constant value in Y direction at larger diameter than about 10 times of testing body depth. The next experiment is to know the wind velocity distribution around the body in order to make clear the reason of the difference of the base pressure distribution in each end plate diameter.

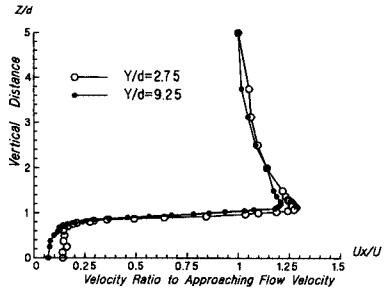

Fig. 7 Vertical distribution of horizontal mean wind velocity of $D/d=4$.

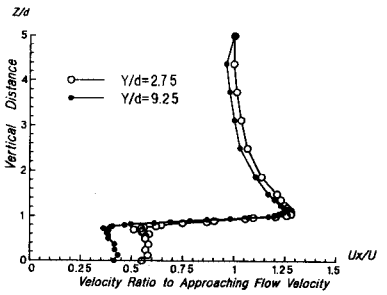

Fig. 8 Vertical distribution of horizontal mean wind velocity of $D/d=10$.

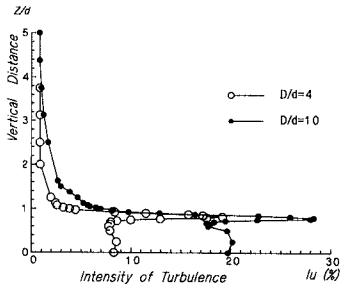

Fig. 9 Vertical distribution of turbulent intensity of horizontal wind velocity of at $X/d=0.625$.

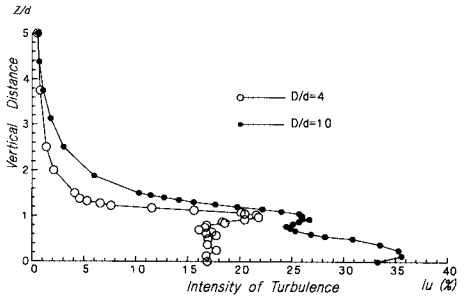

Fig. 10 Vertical distribution of turbulent intensity of horizontal wind velocity of at $X/d=1.5$.

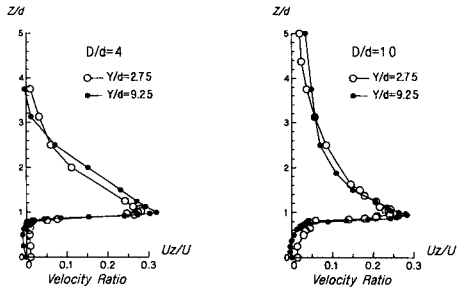

Fig. 11 Vertical distribution of vertical mean wind velocity at $X/d=0.625$.

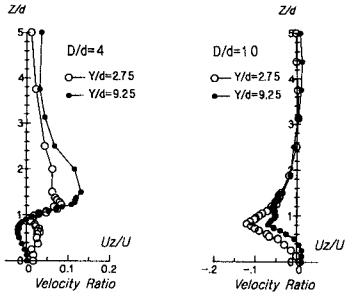

Fig. 12 Vertical distribution of vertical mean wind velocity at $X/d=1.5$

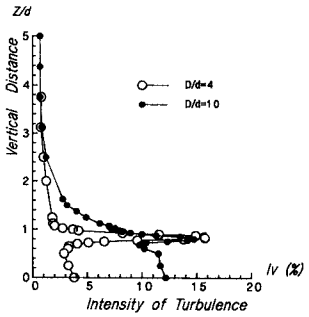

Fig. 13 Vertical distribution of turbulent intensity of vertical wind velocity of at $X/d=0.625$.

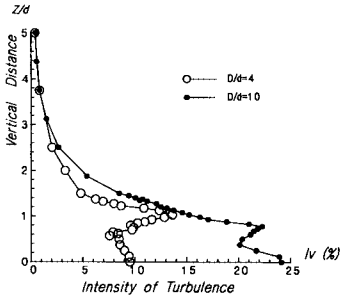

Fig. 14 Vertical distribution of turbulent intensity of vertical wind velocity of at $X/d=1.5$.

6. WIND VELOCITY PROFILES

Figs. 7 and 8 show the vertical wind velocity profile of horizontal component at near the center ($Y/d=2.75$) and near the end plates ($Y/d=9.25$) of the normal flat plate in the cases of the end plate ratio (D/d) of 4 and 10. The significant difference between $D/d=4$ and $D/d=10$ is that the mean wind velocity in the wake of $D/d=4$ is 0.1 times of approaching flow velocity but that of $D/d=10$ is 0.4 times. This means that the mean wind velocities in the wake correspond to the base pressure values of rear surface of the normal flat plate. It seems that there is not significant difference in two dimensional characteristics of wind velocity distributions in the spanwise direction between $D/d=4$ and $D/d=10$, because the horizontal wind velocity distribution at $Y/d<6$ has almost same profile as that at $Y/d=2.75$ for various end plate diameters. According to these results, the loss of two dimensional characteristics of the base pressure distribution in Y direction is considered not to be the main cause for the drastic change of drag forces to the variety of end plate diameters.

Although it is understood from above mentioned figures that the difference of wake flow between two extreme cases is clear, the distribution of intensity of turbulence gives us more detail informations about the wake flow. Figs. 9 and 10 show the vertical distribution of intensity of turbulence of horizontal component of wind velocity in the wake at two points in the flow direction. The magnitude of intensity in the wake of $D/d=10$ is about 2 times of that of $D/d=4$, but those of two cases in the shear layer take near values with increasing the distance in the flow direction.

Figs. 11 to 14 show the vertical component distributions of the mean wind velocity and of the intensity of turbulence behind the testing body. The mean wind velocity distributions are similar in two cases of $D/d=4$ and $D/d=10$ at $X/d=0.625$, but the mean wind velocity in the case of $D/d=10$ has negative values at $X/d=1.5$ and that of $D/d=4$ has almost positive values. The magnitude of intensity of turbulence is almost 70 % of horizontal component in any cases of the diameters and the flow direction distances.

These experimental results teach us that the flow characteristics behind the testing body is inherently different between $D/d=4$ as the end plates of small diameter and $D/d=10$ as that of large diameter and that it is necessary to investigate in more detail by observations of the flow pattern around the testing body by the flow visualization.

7. FLOW VISUALIZATION

The flow patterns were visiualized by hydrogen bubble techniques to make clear the inherent differences between small and large diameter end plates. The water channel with width of 60 cm and length of 20 m was used to visualize the flow patterns by hydrogen bubble techniques. The equipment producing the hydrogen bubble consists of DC-power unit with variable voltage from 0 v to 250 v, pulse generator, 0.03 mm diameter tungsten wire as cathode which produces the hydrogen bubble and lighting system with 4 video lights as shown in Fig. 15. The model for flow visualization was made of acrylic plate of 2 mm thickness. The flat plate has length of 100 mm and depth (d) of 10 mm.

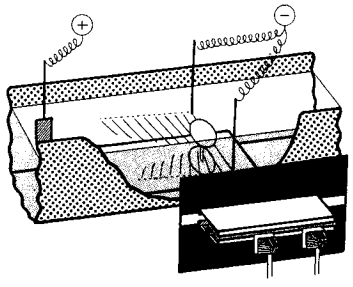

Fig. 15 Flow visualization system.

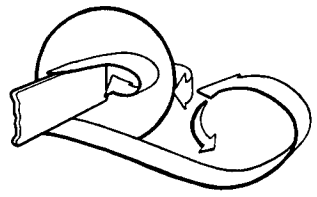

Fig. 16 Illustration of relation between outer flow and wake vortex of normal flat plate with small end plate.

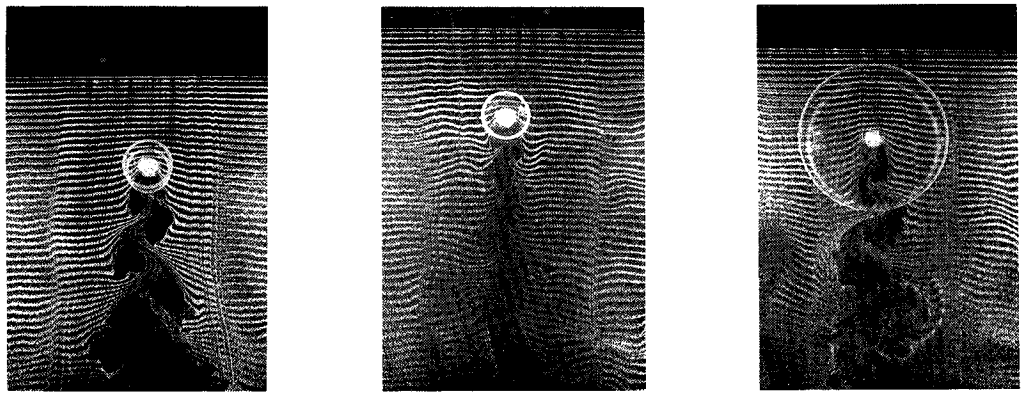

(a) $D/d=4$, center of model axis (b) $D/d=4$, the position of 20 % of model length from end plates (c) $D/d=12$

Photo. 1 Flow patterns observed from model axis.

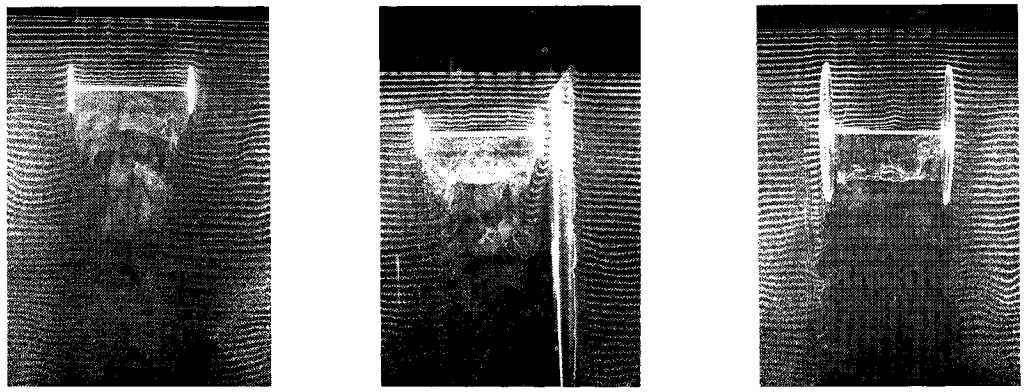

(a) $D/d=4$, without secondary wall (b) $D/d=4$, with secondary wall (c) $D/d=12$

Photo. 2 Flow patterns observed from perpendicular direction to model axis.

Photo. 1 and Photo. 2 were the results of flow visualization, which were taken from y-axis direction and from Z-axis direction, respectively. Photos. 1 (a) and 1 (b) show the flow patterns at the center of the model axis and at the distance of 20 % model length from end plates in the case of $D/d=4$, respectively. The flow pattern of Photo. 1 (a) shows clear vortex formation, but that of Photo. 1 (b) dose not show because the flow at the level of tungsten wire is dragged into model center. The flow characteristics in this case can be seen more clear in the Photo. 2 (a). It can be seen that the outer flows of the end plates have inner direction because of the existence of lower pressure in the wake of the normal flat plate than that their outer region. As the results, the base pressure in the case of small diameter end plates comes to small in absolute value. Adding to this, the vortex formation region near the end plates is larger than that of model center, this corresponds to the base pressure distribution for $D/d=4$ in Fig. 6. On the other hand, the flow pattern of $D/d=12$ shows the same pattern at any part of the model as shown in Photo. 1 (c). This behavior is understood more explicitly from Photo. 2 (c). According to Photo. 2 (c), the separated flow from edges of normal flat plate curls at almost same distance from the edges in whole spanwise. The end plates with larger diameter than the first vortex formation size prevent the occurrence of suction normal to the end plate surfaces. Photo. 2 (b) is the flow visualization for the effect of secondary wall in the case of $D/d=4$. The secondary wall has dimension of $265\times180\times1.5$ mm and the interval of 5 mm between the end plate and the wall. Secondary walls are often used to get rid of the influences from

the boundary layer developed on the wind tunnel walls and the walls are expected the role of end plates, too. But Photo. 2 (c) shows us that the wall seems not to have the role of end plates because even if the existence of the secondary wall, the entrainment of outer flow of the small end plates occurs as similar as the case without the secondary wall. The optimum diameter of end plates is considered to be the larger size than the first vortex formation region, because this size of end plates can prevent the suction normal to them. Fig. 16 illustrates that the outer flow of the end plates is dragged into inner direction by the lower pressure in the wake in the case of the smaller diameter of end plates than the longitudinal length of the first vortex formation region. According to the results of drag coefficient measurement, the optimum size is larger than $D=8\,d$. This size corresponds to the result of von Karman's vortex formation theory, that is, in the case of that vortex interval in flow direction is b and that vortex streets interval is a, the relation between a and b is $a/b=0.28$. It is considered that the center of wake vortex locates at the point of the smallest intensity of wake turbulence. As the first vortex streets interval distance perpendicular to the flow direction in the present case is assumed to be about 1.2 d from Figs. 9 and 10, the vortex interval is calculated as 4.28 d based on von Karman's theory. This value corresponds to $D=8.5\,d$.

8. CONCLUDING REMARKS

The mechanism of end plate effects is investigated by the measurement of drag forces, base pressure distributions, wind velocity profiles and by the flow visualizations. Many important conclusions were taken from above mentioned considerations as the followings.

(1) The Fage & Johansen's experimental data of the normal flat plate has been often used. But according to the present study, it is considered that they used the end plate of diamether of about 6.5 times of depth of the testing body, which is not the optimum size for two dimensional aerostatic force experiments.

(2) Although Maskel reported that the drag force coefficient (C_d) of the normal flat plate is 1.86 after the blockage correction with Fage & Johansen's experimental data, the authors got $C_d=2.108$ by using Maskel's correction equations for the blockage effects to the results of the optimum end plate size.

(3) The role of end plates is to get rid of the flow entrainment from outer region of end plates, which is produced by the negative pressure caused mainly by the nearest wake vortex to the testing body. As the smaller diameter end plates than the optimum size can not prevent the occurrence of the flow entrainment because the negative pressure region is produced out of end plate in the flow direction, it produces the reduction of absolute values of base pressure and reduces the drag forces.

(4) According to the experimental results for the normal flat plate, it can be said that the optimum diameter of end plate is larger than 8 d (d is the depth of the testing body) and this value can be related with von Karman's vortex streets theory.

The recommended end plate size makes it impossible to do the aerodynamic tests because the end plates are too large for dynamic tests. Therefore the correction method for the results of the aerodynamic tests with small end plates should be developed to estimate the true value in wind tunnel tests, for example based on the aerostatic results such as Fig. 5.

The present study is restricted to making clear the role of end plates and measuring the drag forces of the normal flat plate with circular end plates of various diameter, but in the future study, the aerostatic and aerodynamic forces of various bluff-body cylinders and bridge sections with the optimum end plates will be measured and the correction equations will be developed for the experimental results with various end plates in sizes and shapes.

ACKNOWLEDGEMENTS

The authors thank to Professor M. Ito of University of Tokyo, Professor T. Miyata of Yokohama National University and Professor Y. Nakamura of Kyushu University who gave us many precious advises

and comments during accomplishment of the present study.

REFRENCES

1) Nakaguchi, H., Arai, I. and Matsuzaka, M. : Static Wind Loads on Towers of Frame Work Structures, J. of J. S. A. S. S., Vol. 12, No. 121, pp. 29~36, 1964 (in Japanese).
2) Takada, H. : The Experiments on Wake flow of Normal Flat Plates, Proc. of Symposium on Experimental Study of Turbulence, pp. 44~49, 1968 (in Japanse).
3) Fage. A. and Johansen, F. C. : On the flow of Air behind an Inclined Flat Plate of Infinite Span. Proc. Roy. Soc. Proc. (London). ser. A, Vol. 116, No. 773, pp. 170~197, 1927.
4) Maskel, E. C. : A Theory of the Blockage Effects on Bluff Bodies and Stalled Wings in a Closed Wind Tunnel, Aero. Res. Coun. R & M., No. 3400, 1963.
5) Parkinson, G. V. and Jandali, T. : A Wake Source Model for Bluff Body Potential Flow, J. Fluid Mech., Vol. 40, Part 3, pp. 577~594, 1970.
6) Modi, V. J. and El-Sherbiny, S. E. : A Free-Streamline Model for Bluff Bodies in Confined Flow, J. of Fluids Engineering, Trans. of the ASME, pp. 585~592, Sept., 1977.
7) Kubo, Y. and Kato, K. : End Plates Effects and Flow Characteristics around Bluff Body, J. of Wind Engineering, JAWE, No. 24, pp. 37~38, 1985 (in Japanse)
8) Kubo, Y. and Kato, K. : End Plates Effects on Drag Force of Vertical Flat Plates, Memoirs of the Kyushu Institute of Technology, Engineering, No. 15, pp. 1~8, 1985.

(Received September 6 1985)